2 Heat transport in harmonic lattices

If one is interested in a microscopic description of transport through a system, then it is important to model not only the system but also the reservoirs and the system-reservoir couplings. This is known as an open-system description of transport, which is the main theme of Landauer approach. It is quite different from the other popular approaches of transport like the Boltzmann-Peierls transport approach or the Green-Kubo linear response theory, where one studies the properties of the system of only. An idealised reservoir should act as a perfect black body with zero reflectivity. But real experiments do not always depict idealise situation. So it is necessary to achieve a detailed understanding of the role of reservoirs and system-reservoir couplings in transport. Ref. [31] gives a derivation of the basic Landauer results using the Langevin equation approach, both for electrons and phonons. In Sec.(2.1), we introduce and discuss the method of generalised Langevin equations and Green's function (LEGF), and derive exact expressions for the heat current in harmonic lattices. These expressions are of identical form as those obtained from the nonequilibrium Green's function (NEGF) formalism. We work out the non-equilibrium steady state properties of a harmonic lattice which is connected to heat reservoirs at different temperatures [33]. The heat reservoirs themselves are modeled as harmonic systems. Our approach is to write quantum Langevin equations for the system and solve these to obtain steady state properties such as currents and other second moments involving the position and the momentum operators.

In latter Secs.(2.2,2.3) we discuss two applications of the LEGF approach to transport. We consider heat conduction in a harmonic chain connected to self-consistent Ohmic heat reservoirs [33]. The temperatures of the two heat baths at the boundaries are specified from before, whereas the temperatures of the interior heat reservoirs are determined self-consistently by demanding that in the steady state, on an average, there is no heat current between any such (self-consistent) reservoir and the harmonic chain. We obtain a temperature-dependent thermal conductivity which, in the high-temperature classical limit, reproduces the exact result on this model obtained recently by Bonetto, Lebowitz and Lukkarinen [40]. We also demonstrate the crossover from ballistic to diffusive thermal transport in the finite harmonic chain by changing the strength of coupling of the interior Ohmic heat reservoirs to the chain sites [41]. The main feature of our study is that the effective mean free path separating the ballistic regime of transport from the diffusive one emerges naturally. The other application [Sec.(2.3)] is on heat transport in ordered harmonic lattices with tunable boundary conditions [42]. In the classical case, we derive an exact

formula for the heat current in the limit of system size $N \to \infty$. In some special cases this reproduces earlier results obtained by Rieder, Lebowitz and Lieb (RLL) [43] and by Nakazawa [44, 45] using different methods. We also obtain results for the quantum mechanical case where we study the temperature dependence of the heat current. Finally we briefly state results in higher dimensions.

2.1 Langevin equations and Green's function formalism (LEGF) for thermal transport

The harmonic crystal is one of the the simplest model that one learns in solid state physics and it is known to reproduce correctly, for example, some of the experimental features of the specific heat of an insulating solid. The harmonic approximation basically involves expanding the full atomic potential of the solid about its minimum (which one assumes is a crystal) and keeping terms up to second order. If one transforms to normal mode coordinates, then the harmonic crystal can be viewed as a collection of noninteracting phonons. While many equilibrium properties can be understood satisfactorily within the harmonic approximation, transport properties (heat conduction) of the harmonic lattice are anomalous because of the absence of interactions between the phonons.

In this section we discuss a formalism for transport in harmonic lattices based on the Langevin equation approach [33]. This approach was first used to study heat conduction in a one-dimensional ordered harmonic lattice [43]. Subsequently, this approach was used to study heat conduction in disordered harmonic lattices in one [16, 18, 46] and two dimensions [47]. Later, in Chapter (4) we will use this approach for further studies in disordered phononic systems. The quantum mechanical case has also been studied by several authors [31, 48–53] using an open system description either through quantum Langevin equations or through density matrices. The open system description for harmonic systems closely resembles the Landauer formalism used for electron transport. Another rigorous approach to studying electron transport in mesoscopic systems is the NEGF [54], and Ref. [32] shows how this can be derived, for non-interacting electrons modeled by tight-binding Hamiltonians, using a quantum Langevin equation approach. We note that the Landauer formalism has also been discussed in the context of wave propagation in disordered media [55, 56]. The problems of heat conduction in disordered harmonic lattices and wave propagation in disordered media are closely related. It is expected that some of the work in the latter area, for example, on localization, will be useful in the context of heat conduction.

In our paper [33], we show how the LEGF method for harmonic lattices leads to NEGF-like expressions for phonon transport. For simplicity, we restrict ourselves to harmonic Hamiltonians

with scalar displacement variables at each lattice site. It is straightforward to extend the calculations to the case of vector displacements. The basic steps in the calculation are: (i) one thinks of the full system as consisting of the sample we are interested in (henceforth called wire) as well as the reservoirs at different temperatures which are connected to the wire, (ii) the wire and the reservoir Hamiltonians are taken to be harmonic, (iii) we eliminate the reservoir degrees of freedom and this leads to Langevin equations of motion for the wire variables, (iv) the linear Langevin equations are solved and steady state properties such as expectation values of the current are found. Finally (v) the solution is written in a form where one can identify the usual phonon Green's functions, commonly used in solid state physics. This leads to the identification with results from the NEGF formalism. We note that Landauer-like results for phonons have been proposed earlier [57, 58] and some recent papers [59, 60] derive NEGF results for phonon transport using the Keldysh approach.

2.1.1 Quantum Langevin equations

We consider a harmonic system which consists of a wire (denoted by W) coupled to reservoirs which are also described by harmonic interactions. In most of our discussions we consider the case of two reservoirs, labeled as L (for left) and R (right) , which are at two different temperatures. It is easy to generalize the case where there are more than two reservoirs. The Hamiltonian of the entire system of wire and reservoirs is taken to be

$$\begin{aligned}
\mathcal{H} &= \frac{1}{2}\dot{X}^T M \dot{X} + \frac{1}{2} X^T \Phi X \qquad (2.1)\\
&= \mathcal{H}_W + \mathcal{H}_L + \mathcal{H}_R + \mathcal{V}_L + \mathcal{V}_R \\
\text{where}\quad \mathcal{H}_W &= \frac{1}{2}\dot{X}_W^T M_W \dot{X}_W + \frac{1}{2} X_W^T \Phi_W X_W \ , \\
\mathcal{H}_L &= \frac{1}{2}\dot{X}_L^T M_L \dot{X}_L + \frac{1}{2} X_L^T \Phi_L X_L \ , \\
\mathcal{H}_R &= \frac{1}{2}\dot{X}_R^T M_R \dot{X}_R + \frac{1}{2} X_R^T \Phi_R X_R \ , \\
\mathcal{V}_L &= X_W^T V_L X_L, \quad \mathcal{V}_R = X_W^T V_R X_R \ ,
\end{aligned}$$

where $M,\ M_W,\ M_L,\ M_R$ are real diagonal matrices representing masses of the particles in the entire system, wire, left, and right reservoirs respectively. The quadratic potential energies are given by the real symmetric matrices $\Phi,\ \Phi_W,\ \Phi_L,\ \Phi_R$ while V_L and V_R denote the interaction between the wire and the two reservoirs. The column vectors $X,\ X_W,\ X_L,\ X_R$ are Heisenberg operators which correspond to particle displacements, assumed to be scalars, about some equilibrium configuration. Thus $X = \{X_1, X_2, ...X_{N_s}\}^T$ where X_r denotes the position operator of the r^{th} particle and N_s denotes the number of points in the entire system. Also $\dot{X} = M^{-1}\ P$ where P_r denotes the momentum operator, with $\{X_r,\ P_r\}$ satisfying the usual commutation relations $[X_r, P_s] = i\hbar\delta_{rs}$.

The Heisenberg equations of motion for the system are:

$$M_W \ddot{X}_W = -\Phi_W X_W - V_L X_L - V_R X_R \ , \tag{2.2}$$

and the equations of motion for the two reservoirs are

$$\begin{aligned} M_L \ddot{X}_L &= -\Phi_L X_L - V_L^T X_W \ , & (2.3)\\ M_R \ddot{X}_R &= -\Phi_R X_R - V_R^T X_W \ . & (2.4) \end{aligned}$$

We solve these equations by considering them as linear inhomogeneous equations. Thus for the left reservoir the general solution to Eq. (2.3) is (for $t > t_0$):

$$\begin{aligned} X_L(t) &= f_L^+(t-t_0) M_L X_L(t_0) + g_L^+(t-t_0) M_L \dot{X}_L(t_0) \\ &\quad - \int_{t_0}^{t} dt' \ g_L^+(t-t') V_L^T X_W(t') \ , \qquad (2.5)\\ \text{with} \quad f_L^+(t) &= U_L \cos(\Omega_L t) U_L^T \ \theta(t), \quad g_L^+(t) = U_L \frac{\sin(\Omega_L t)}{\Omega_L} U_L^T \ \theta(t) \ , \end{aligned}$$

where $\theta(t)$ is the Heaviside function and $U_L,\ \Omega_L$ are the normal mode eigenvector and eigenvalue matrices respectively and which satisfy the equations:

$$U_L^T \Phi_L U_L = \Omega_L^2 \ , \quad U_L^T M_L U_L = I \ .$$

Similarly, for the right reservoir we obtain

$$\begin{aligned} X_R(t) &= f_R^+(t-t_0) M_R X_R(t_0) + g_R^+(t-t_0) M_R \dot{X}_R(t_0) \\ &\quad - \int_{t_0}^{t} dt' \ g_R^+(t-t') V_R^T X_W(t') \ . \qquad (2.6) \end{aligned}$$

We plug these solutions back into the equation of motion for the system to get

$$\begin{aligned} M_W \ddot{X}_W &= -\Phi_W X_W \ + \ \eta_L \ + \ \int_{t_0}^{t} dt' \ V_L \ g_L^+(t-t') \ V_L^T \ X_W(t') \\ &\quad + \eta_R \ + \ \int_{t_0}^{t} dt' \ V_R \ g_R^+(t-t') \ V_R^T \ X_W(t') \ , \qquad (2.7) \end{aligned}$$

where

$$\begin{aligned} \eta_L &= -V_L \ [f_L^+(t-t_0) M_L X_L(t_0) \ + \ g_L^+(t-t_0) M_L \dot{X}_L(t_0)] \\ \eta_R &= -V_R \ [f_R^+(t-t_0) M_R X_R(t_0) \ + \ g_R^+(t-t_0) M_R \dot{X}_R(t_0)] \ . \qquad (2.8) \end{aligned}$$

This equation has the form of a quantum Langevin equation. The properties of the noise terms η_L and η_R are determined using the condition that, at time t_0, the two isolated reservoirs are described

by equilibrium phonon distribution functions. At time t_0 the left reservoir is in equilibrium at temperature T_L and the population of the normal modes (of the isolated left reservoir) is given by the distribution function $f_b(\omega, T_L) = 1/[e^{\hbar\omega/k_B T_L} - 1]$. The equilibrium correlations are then given by:

$$\begin{aligned}
\langle X_L(t_0) X_L^T(t_0)\rangle &= U_L \frac{\hbar}{2\Omega_L} \coth\left(\frac{\hbar\Omega_L}{2k_B T_L}\right) U_L^T \ , \\
\langle \dot{X}_L(t_0) \dot{X}_L^T(t_0)\rangle &= U_L \frac{\hbar\Omega_L}{2} \coth\left(\frac{\hbar\Omega_L}{2k_B T_L}\right) U_L^T \\
\langle X_L(t_0) \dot{X}_L^T(t_0)\rangle &= U_L \left(\frac{i\hbar}{2}\right) U_L^T \\
\langle \dot{X}_L^T(t_0) X_L(t_0)\rangle &= U_L \left(\frac{-i\hbar}{2}\right) U_L^T \ .
\end{aligned}$$

Using these we can determine the correlations of the noise terms in Eq. (2.8). Thus we get for the left reservoir noise correlations:

$$\begin{aligned}
\langle \eta_L(t) \eta_L^T(t')\rangle &= V_L U_L \left[\cos\Omega_L(t-t') \frac{\hbar}{2\Omega_L} \coth\left(\frac{\hbar\Omega_L}{2k_B T_L}\right)\right. \\
&\qquad \left. -i \sin\Omega_L(t-t') \frac{\hbar}{2\Omega_L}\right] U_L^T V_L^T \ , \qquad (2.9)
\end{aligned}$$

and a similar expression for the right reservoir.

2.1.2 Stationary solution of the equations of motion

Now let us take the limits of infinite reservoir sizes and let $t_0 \to -\infty$. We can then solve Eq. (2.7) by taking Fourier transforms. Thus defining the Fourier transforms

$$\begin{aligned}
\tilde{X}_W(\omega) &= \frac{1}{2\pi} \int_{-\infty}^{\infty} dt \ X_W(t) e^{i\omega t} \ , \\
\tilde{\eta}_{L,R}(\omega) &= \frac{1}{2\pi} \int_{-\infty}^{\infty} dt \ \eta_{L,R}(t) e^{i\omega t} \ , \\
g^+_{L,R}(\omega) &= \int_{-\infty}^{\infty} dt \ g^+_{L,R}(t) e^{i\omega t} \ , \qquad (2.10)
\end{aligned}$$

we get from Eq. (2.7)

$$\begin{aligned}
(-\omega^2 \ M_W + \Phi_W)\tilde{X}_W(\omega) &= [\ \Sigma_L^+(\omega) + \Sigma_R^+(\omega)\ ]\ \tilde{X}_W(\omega) + \tilde{\eta}_L(\omega) + \tilde{\eta}_R(\omega) \\
\text{where} \quad \Sigma_L^+(\omega) &= V_L g_L^+(\omega) V_L^T, \quad \Sigma_R^+(\omega) = V_R g_R^+(\omega) V_R^T \ . \qquad (2.11)
\end{aligned}$$

The noise correlations can be obtained from Eq. (2.9) and we get (for the left reservoir):

$$\begin{aligned}
\langle \tilde{\eta}_L(\omega) \tilde{\eta}_L^T(\omega')\rangle &= \delta(\omega+\omega') \ V_L \ Im[g_L^+(\omega)] \ V_L^T \ \frac{\hbar}{\pi}[1 + f_b(\omega, T_L)] \\
&= \delta(\omega+\omega') \ \Gamma_L(\omega) \ \frac{\hbar}{\pi}[1 + f_b(\omega, T_L)] \qquad (2.12) \\
&\quad \text{where} \quad \Gamma_L(\omega) = Im[\Sigma_L^+(\omega)] \qquad (2.13)
\end{aligned}$$

which is a fluctuation-dissipation relation. This also leads to the more commonly used correlation:

$$\frac{1}{2}\langle\ \tilde{\eta}_L(\omega)\tilde{\eta}_L^T(\omega') + \tilde{\eta}_L(\omega')\tilde{\eta}_L^T(\omega)\ \rangle = \delta(\omega+\omega')\ \Gamma_L(\omega)\ \frac{\hbar}{2\pi}\ \coth(\frac{\hbar\omega}{2k_BT_L}). \tag{2.14}$$

Similar relations hold for the noise from the right reservoir. We then get the following stationary solution to the equations of motion:

$$\begin{aligned} X_W(t) &= \int_{-\infty}^{\infty} d\omega \tilde{X}_W(\omega) e^{-i\omega t}\ , \\ \text{with}\quad \tilde{X}_W(\omega) &= G_W^+(\omega)\ [\tilde{\eta}_L(\omega) + \tilde{\eta}_R(\omega)]\ , \qquad (2.15) \\ \text{where}\quad G_W^+ &= \frac{1}{[-\omega^2 M_W + \Phi_W - \Sigma_L^+(\omega) - \Sigma_R^+(\omega)]}\ . \qquad (2.16) \end{aligned}$$

The identification of $G_W^+(\omega)$ as a phonon Green function, with $\Sigma_{L,R}^+(\omega)$ as effective self energy terms, is the main step that enables a comparison of results derived by the quantum Langevin approach with those obtained from the NEGF method. In Appendix A.1, we show explicitly how this identification is made.

For the reservoirs we get, from Eqs. (2.5-2.6),

$$\begin{aligned} -V_L\tilde{X}_L(\omega) &= \tilde{\eta}_L(\omega) + \Sigma_L^+\tilde{X}_W(\omega)\ , \\ -V_R\tilde{X}_R(\omega) &= \tilde{\eta}_R(\omega) + \Sigma_R^+\tilde{X}_W(\omega)\ . \end{aligned} \tag{2.17}$$

2.1.3 Steady state properties

Current: The simplest way to evaluate the steady state current is to evaluate the following expectation value for left-to-right current:

$$J = -\langle\ \dot{X}_W^T V_L X_L\ \rangle = \int_{-\infty}^{\infty} d\omega \int_{-\infty}^{\infty} d\omega'\ e^{-i(\omega+\omega')t} i\omega\ \langle \tilde{X}_W^T(\omega) V_L \tilde{X}_L(\omega')\rangle\ ,$$

which is just the rate at which the left reservoir does work on the wire. Using the solution in Eq. (2.15-2.17) we get

$$\begin{aligned} J &= -\int_{-\infty}^{\infty} d\omega \int_{-\infty}^{\infty} d\omega'\ e^{-i(\omega+\omega')t} i\omega\ \langle\ (\ \tilde{\eta}_L^T(\omega) + \tilde{\eta}_R^T(\omega)\ )\ {G_W^+}^T(\omega) \\ &\quad \times [\ \tilde{\eta}_L(\omega') + \Sigma_L^+(\omega')\ G_W^+(\omega')\ (\ \tilde{\eta}_L(\omega') + \tilde{\eta}_R(\omega')\ )\ ]\ \rangle\ . \end{aligned} \tag{2.18}$$

Now consider that part of J, say J^R, which depends only on T_R. Clearly this is:

$$\begin{aligned} J^R &= -\int_{-\infty}^{\infty} d\omega \int_{-\infty}^{\infty} d\omega'\ e^{-i(\omega+\omega')t}\ i\ \omega \\ &\quad \times Tr\ [\ {G_W^+}^T(\omega)\ \Sigma_L^+(\omega')\ G_W^+(\omega')\ \langle\ \tilde{\eta}_R(\omega')\tilde{\eta}_R^T(\omega)\ \rangle\ ] \\ &= -\ i\int_{-\infty}^{\infty} d\omega\ Tr[\ {G_W^+}^T(\omega)\ \Sigma_L^+(-\omega) G_W^+(-\omega)\Gamma_R(\omega)]\ \frac{\hbar\omega}{\pi}\ [1 + f_b(\omega, T_R)]\ . \end{aligned}$$

Using the identities ${G_W^+}^T = G_W^+$, $G_W^+(-\omega) = G_W^-(\omega)$ and taking the real part of above equation we obtain, after some simplifications,

$$J^R = -\int_{-\infty}^{\infty} d\omega \; Tr[\; G_W^+(\omega)\; \Gamma_L(\omega)\; G_W^-(\omega)\; \Gamma_R(\omega)\;]\; \frac{\hbar\omega}{\pi}\; [1 + f_b(\omega, T_R)]\; .$$

Including the contribution from the terms involving T_L, and noting that the current has to vanish for $T_L = T_R$, it is clear that the net current will be given by

$$J = \int_{-\infty}^{\infty} d\omega \; Tr[\; G_W^+(\omega)\; \Gamma_L(\omega) G_W^-(\omega)\; \Gamma_R(\omega)]\; \frac{\hbar\omega}{\pi}\; [f(\omega, T_L) - f(\omega, T_R)]\; . \tag{2.19}$$

This expression for current can be seen to be of identical form as the NEGF expression for electron current (see for example [54, 61, 62]).

Two point correlation functions: We can also easily compute expectation values of various correlations. Thus the velocity-velocity correlations are given by

$$\begin{aligned} K &= \langle \dot{X}_W \dot{X}_W^T \rangle \\ &= \int_{-\infty}^{\infty} d\omega\; \frac{\omega}{\pi}\; [\; G_W^+(\omega)\Gamma_L(\omega)G_W^-(\omega)\hbar\omega(1 + f_b(\omega, T_L)) \\ &\qquad + G_W^+(\omega)\Gamma_R(\omega)G_W^-(\omega)\hbar\omega(1 + f_b(\omega, T_R))\;] \\ &= \int_{-\infty}^{\infty} d\omega \frac{\omega}{\pi}\; [\; G_W^+(\omega)\Gamma_L(\omega)G_W^-(\omega)\frac{\hbar\omega}{2}\coth(\frac{\hbar\omega}{2k_B T_L}) \\ &\qquad + G_W^+(\omega)\Gamma_R(\omega)G_W^-(\omega)\frac{\hbar\omega}{2}\coth(\frac{\hbar\omega}{2k_B T_R})\;]\; , \end{aligned} \tag{2.20}$$

where the last line is easily obtained after writing $K = (K + K^*)/2$. We see that for $T_L = T_R$ this reduces to the equilibrium result of Eq. (A.10) *provided that there are no bound states*.

Similarly the position-position and position-velocity correlations are given by:

$$\begin{aligned} P &= \langle X_W X_W^T \rangle \\ &= \int_{-\infty}^{\infty} d\omega \frac{\hbar}{2\pi}\; [\; G_W^+(\omega)\Gamma_L(\omega)G_W^-(\omega)\coth(\frac{\hbar\omega}{2k_B T_L}) \\ &\qquad + G_W^+(\omega)\Gamma_R(\omega)G_W^-(\omega)\coth(\frac{\hbar\omega}{2k_B T_R})\;]\; , \\ C &= \langle X_W \dot{X}_W^T \rangle \\ &= \int_{-\infty}^{\infty} d\omega \frac{i}{\pi}\; [\; G_W^+(\omega)\Gamma_L(\omega)G_W^-(\omega)\frac{\hbar\omega}{2}\coth(\frac{\hbar\omega}{2k_B T_L}) \\ &\qquad + G_W^+(\omega)\Gamma_R(\omega)G_W^-(\omega)\frac{\hbar\omega}{2}\coth(\frac{\hbar\omega}{2k_B T_R})\;]\; . \end{aligned} \tag{2.21}$$

The correlation functions K and P can be used to define the local energy density which can in turn be used to define the temperature profile in the non-equilibrium steady state of the wire.

Also we note that the correlations C give the local heat current density. In the next section we will find that it is sometimes more convenient to evaluate the total steady state current from this expression rather than the one in Eq. (2.19).

Classical limits: The classical limit is obtained by taking the high temperature limit so that $\hbar\omega/k_BT \to 0$. Then we obtain the following expressions for the various steady state properties computed in the last section. The current is given by

$$J = \frac{k_B\ (T_L - T_R)}{\pi}\ \int_{-\infty}^{\infty} d\omega\ Tr[\ G_W^+(\omega)\ \Gamma_L(\omega) G_W^-(\omega)\ \Gamma_R(\omega)]\ , \tag{2.22}$$

while other correlation functions are given by:

$$\begin{aligned}
K &= \frac{k_BT_L}{\pi}\int_{-\infty}^{\infty} d\omega\ \omega\ G_W^+(\omega)\Gamma_L(\omega)G_W^-(\omega) \\
&\quad + \frac{k_BT_R}{\pi}\int_{-\infty}^{\infty} d\omega\ \omega\ G_W^+(\omega)\Gamma_R(\omega)G_W^-(\omega)\ , \\
P &= \frac{k_BT_L}{\pi}\int_{-\infty}^{\infty} d\omega\ \frac{1}{\omega}\ G_W^+(\omega)\Gamma_L(\omega)G_W^-(\omega) \\
&\quad + \frac{k_BT_R}{\pi}\int_{-\infty}^{\infty} d\omega\ \frac{1}{\omega}\ G_W^+(\omega)\Gamma_R(\omega)G_W^-(\omega)\ , \\
C &= \frac{ik_BT_L}{\pi}\int_{-\infty}^{\infty} d\omega\ G_W^+(\omega)\Gamma_L(\omega)G_W^-(\omega) \\
&\quad + \frac{ik_BT_R}{\pi}\int_{-\infty}^{\infty} d\omega\ G_W^+(\omega)\Gamma_R(\omega)G_W^-(\omega)\ .
\end{aligned} \tag{2.23}$$

For one dimensional wires these lead to [31] expressions for current and temperature used in earlier studies of heat conduction in disordered harmonic chains [16, 18, 46].

2.1.4 Discussion

In this section, using the quantum LEGF approach, we have derived NEGF-like expressions for the heat current in a harmonic lattice connected to external reservoirs at different temperatures [33]. We note that unlike other approaches such as the Green-Kubo formalism and Boltzmann equation approach, the LEGF approach explicitly includes the reservoirs. The Langevin equation is also physically appealing since it gives a nice picture of the reservoirs as sources of noise and dissipation. Also, just as the Landauer formalism and NEGF have been extremely useful in understanding electron transport in mesoscopic systems it is likely that a similar description will be useful for the case of heat transport in insulating nanotubes, nanowires, etc. We note here that the single-channel Landauer results follow from NEGF if one considers one-dimensional reservoirs [31] and have been useful in interpreting experimental results [63].

We think that the similarity between heat conduction studies in harmonic systems and electron transport in noninteracting wires is an interesting and useful point to note. The two areas

have developed quite independently using different theoretical tools. In the former case most of the earlier studies were done on classical systems using either a Langevin or a Fokker Planck description. More recent studies on quantum systems have used either a quantum Langevin or a density matrix approach. On the other hand, for the electron case, which is inherently quantum-mechanical, the most popular and useful approach has been the Landauer and the NEGF formalism. As we have demonstrated, in this paper for the phonon case, and in Ref [32] for the electron case, the NEGF results can be easily derived using the Langevin approach, at least in the noninteracting case.

The LEGF approach has some advantages. For example, in the classical heat conduction case, it is easy to write Langevin equations for nonlinear systems and study them numerically. Also they might be useful in studying time dependent phenomena. Examples of this are the treatment of quantum pumping in [64] and the treatment of the question of approach to the non-equilibrium steady state in [32]. We feel that it is worthwhile to explore the possibility of using the quantum LEGF approach to the harder and more interesting problems involving interactions and time-dependent potentials in both the electron and the phonon case.

2.2 One-dimensional harmonic crystal with self-consistent heat baths

As an application of the LEGF formalism, we consider the problem of heat transport in a harmonic chain with each site connected to self-consistent heat reservoirs [33, 41]. The classical version of this model was first studied by [20, 21] where the authors introduced the self-consistent reservoirs as a simple scattering mechanism which might ensure local equilibration and the validity of Fourier's law. We recall that Fourier's law states that for a solid with a spatially varying temperature field $T(\mathbf{x})$ inside it, the local heat current density $\mathbf{J}$ at a point $\mathbf{x}$ is given by:

$$\mathbf{J}(\mathbf{x}) = -\kappa \nabla T(\mathbf{x}) \tag{2.24}$$

where κ defines the thermal conductivity of the solid and is expected to be an intrinsic property of the material. Fourier's law is a phenomenological law which is expected to be true in the hydrodynamic linear response regime. However, till now, there does not exist any purely mechanical model (without external potentials) in which a first principle demonstration of the validity of Fourier's law, either numerically or analytically, has been achieved.

Infact it is now pretty much clear that in one-dimensional momentum conserving systems, Fourier's law is not valid and one cannot define a system-size independent thermal conductivity for these systems [66–74] (Note that the momentum referred to here is the total real momentum, and not the crystal momentum. This is conserved if there are no external potentials). Apart

from a large number of numerical studies, various theoretical approaches have been used for different classes of systems to arrive at this conclusion regarding non-validity of Fourier's law in one dimension. In the case of interacting systems (nonlinear), the anomalous behaviour of thermal conductivity has been understood within the Green-Kubo formalism and has been related to long-time tails in the current-current auto-correlation functions [73, 74]. For non-interacting (harmonic) disordered systems, heat transport occurs through independent phonon modes and the main contribution comes from low frequency extended modes [18].

This self-consistent reservoir model was recently solved exactly by Bonetto $et\ \ al.$ [40] who proved local equilibration and validity of Fourier's law and obtained an expression for the thermal conductivity of the wire. They also showed that the temperature profile in the wire was linear. The quantum version of the problem was also studied by Visscher and Rich [22] who analyzed the limiting case of weak coupling to the self-consistent reservoirs. We will show here how the present formalism can be used to obtain results in the quantum-mechanical case. The classical results of Bonetto $et\ al.$ are obtained as the high temperature limit, while the quantum mechanical results of Vischer and Rich are obtained in the weak coupling limit.

In this model one considers a one-dimensional harmonic wire described by the Hamiltonian

$$\begin{aligned} H_W &= \sum_{l=1}^{N} \frac{m}{2}[\dot{x}_l^2 + \omega_0^2 x_l^2] + \sum_{l=1}^{N+1} \frac{m\omega_c^2}{2}(x_l - x_{l-1})^2 \ , \\ &= \frac{1}{2}\dot{X}_W^T M_W \dot{X}_W + \frac{1}{2} X_W^T \Phi_W X_W \end{aligned} \tag{2.25}$$

where the wire particles are denoted as $X^T = \{x_1, x_2, ...x_N\}$ and we have chosen the boundary conditions $x_0 = x_{N+1} = 0$. All the particles are connected to heat reservoirs which are taken to be Ohmic. The coupling strength to the reservoirs is controlled by the dissipation constant γ. The temperatures of the first and last reservoirs are fixed and taken to be $T_1 = T_L$ and $T_N = T_R$. For other particles, *i.e* $l = 2, 3...(N-1)$, the temperature of the attached reservoir T_l is fixed self-consistently in such a way that the net current flowing into any of the reservoirs $l = 2, 3...(N-1)$ vanishes. The Langevin equations of motion for the particles on the wire are:

$$m\ddot{x}_l = -m\omega_c^2(2x_l - x_{l-1} - x_{l+1}) - m\omega_0^2 x_l - \gamma\dot{x}_l + \eta_l \quad l = 1, 2...N \ , \tag{2.26}$$

where the noise-noise correlation is easier to express in frequency domain and given by

$$\frac{1}{2}\langle\ \eta_l(\omega)\eta_m(\omega') + \eta_l(\omega')\eta_m(\omega)\ \rangle = \frac{\gamma\hbar\omega}{2\pi}\coth(\frac{\hbar\omega}{2k_B T_l})\ \delta(\omega+\omega')\ \delta_{lm} \ . \tag{2.27}$$

From the equations of motion it is clear that the l^{th} particle is connected to a bath with a self energy matrix $\Sigma_l^+(\omega)$ whose only non vanishing element is $[\Sigma_l^+]_{ll} = i\gamma\omega$. Generalizing Eq. (2.19) to the case of multiple baths we find that the heat current from the l^{th} reservoir into the wire is

given by:

$$J_l = \sum_{m=1}^{N} \int_{-\infty}^{\infty} d\omega \; Tr[\; G_W^+(\omega) \; \Gamma_l(\omega) G_W^-(\omega) \; \Gamma_m(\omega)] \frac{\hbar\omega}{\pi} \; [f(\omega, T_l) - f(\omega, T_m)] \; , \quad (2.28)$$
$$\text{where} \quad G_W^+ = [\; -\omega^2 \; M_W + \Phi_W - \sum_l \Sigma_l^+(\omega) \;]^{-1} \; , \quad \Gamma_l = Im[\Sigma_l^+] \; .$$

Using the form of Γ_l we then get:

$$J_l = \sum_{m=1}^{N} \gamma^2 \; \int_{-\infty}^{\infty} d\omega \; \omega^2 \mid [G_W^+(\omega)]_{lm} \mid^2 \; \frac{\hbar\omega}{\pi} \; [f(\omega, T_l) - f(\omega, T_m)] \; .$$

To find the temperature profile we need to solve the $N-2$ nonlinear equations $J_l = 0$ for $l = 2, 3...N-1$ with $T_1 = T_L$ and $T_N = T_R$. To proceed we consider the linear response regime with the applied temperature difference $\Delta T = T_L - T_R << T$ where $T = (T_L + T_R)/2$. In that case we expand the phonon distribution functions $f(\omega, T_l)$ about the mean temperature T and get the following simpler expressions for the currents

$$J_l = \gamma^2 \; \int_{-\infty}^{\infty} d\omega \; \frac{\hbar\omega^3}{\pi} \frac{\partial f(\omega, T)}{\partial T} \; \sum_{m=1}^{N} \; \mid [G_W^+(\omega)]_{lm} \mid^2 \; (T_l - T_m) \; . \quad (2.29)$$

We write $G^+ = Z^{-1}/(m\omega_c^2)$ where Z is a tridiagonal matrix with offdiagonal elements equal to -1 and diagonal elements are all equal to $z = 2 + \omega_0^2/\omega_c^2 - \omega^2/\omega_c^2 - i\gamma\omega/(m\omega_c^2)$. It is then easy to find its inverse using the formula $Z_{lm}^{-1} = D_{1,l-1} \; D_{m+1,N}/D_{1,N}$, where D_{ij} is the determinant of the sub-matrix of Z beginning with the ith row and column and ending with the jth row and column. The determinant is given by $D_{ij} = \sinh[(j-i+2) \; \alpha]/\sinh(\alpha)$, where $e^\alpha = z/2 \pm [(z/2)^2 - 1]^{1/2}$ (any of the two roots can be taken). For points far from the boundaries of the wire ($l = yN$ where $y = O(1), \; 1-y = O(1)$) we then find that

$$G_{lm}^+ = \frac{e^{-\alpha|l-m|}}{2m\omega_c^2 \sinh\alpha} \; , \quad (2.30)$$

where we choose the root α such that $\alpha_R = Re[\alpha] > 0$.

2.2.1 Infinite chain:

In Ref. [40], where the classical version of the present model was studied, it was shown that in the limit $N \to \infty$ the temperature profile obtained by solving the self-consistent equations has the linear form

$$T_l = T_L + \frac{l-1}{N-1}(T_R - T_L) \; . \quad (2.31)$$

From the form of G^+_{lm} in Eq. (2.30) we see at once that, for any point l in the bulk of the wire, the zero-current condition $J_l = 0$ is satisfied since $\sum_{m=-\infty}^{\infty}(l-m)|e^{-\alpha|l-m|}|^2 = 0$. For points which are within distance $O(1)$ from the boundaries the temperature profile deviates from the linear form.

To find the net left-right current in the wire we could use the formula for $J_1 = -J_N$ given in Eq. (2.40). However we notice that use of this formula requires us to know the accurate form of T_m for points m close to the boundaries since these terms contribute significantly to the sum in Eq. (2.40). We instead use a different expression for the current. We evaluate the left-right current $J_{l,l+1}$ on the bond connecting sites l and $(l+1)$. Using Eq. (2.21) and in the linear response limit, making expansions about T, we get

$$\begin{aligned} J_{l,\ l+1} &= m\omega_c^2\ \langle x_l \dot{x}_{l+1}\rangle = -\frac{m\omega_c^2\gamma}{\pi}\int_{-\infty}^{\infty} d\omega\ \omega\ \left(\frac{\hbar\omega}{2k_BT}\right)^2 \mathrm{cosech}^2(\frac{\hbar\omega}{2k_BT}) \\ &\quad \times \sum_{m=1}^{N} k_BT_m\ Im\{[G^+_W(\omega)]_{lm}[G^+_W(\omega)]^*_{l+1\ m}\}\ . \end{aligned} \tag{2.32}$$

The current value is independent of l and we choose to evaluate it at a value of l in the bulk of the wire. In that case terms in the sum above which contain T_m with m close to the boundaries are exponentially small ($\sim e^{-\alpha N}$) and so do not contribute. Hence we can use the linear temperature profile for T_m and the form of G^+_W in Eq. (2.30) to evaluate the heat current. We get:

$$\begin{aligned} J &= -\frac{\gamma}{8m\omega_c^2\pi i}\int_{-\infty}^{\infty} d\omega\ \frac{\omega}{|\sinh\alpha|^2}\ \left(\frac{\hbar\omega}{2k_BT}\right)^2 \mathrm{cosech}^2(\frac{\hbar\omega}{2k_BT}) \\ &\quad \times \sum_{m=-\infty}^{\infty} k_BT_m\ [e^{-\alpha|l-m|}e^{-\alpha^*|l+1-m|} - e^{-\alpha^*|l-m|}e^{-\alpha|l+1-m|}]\ , \end{aligned}$$

where the additional terms in the summation over m are exponentially small contributions. Also as before we choose the root $\alpha(\omega)$ such that $Re[\alpha] > 0$. Using the notation $\alpha_R(\omega) = Re[\alpha],\ \alpha_I(\omega) = Im[\alpha]$ we get, after some algebra, the following expression for the thermal conductivity $\kappa = JN/\Delta T$ (obtained in the large N limit):

$$\kappa = \frac{\gamma k_B}{16m\omega_c^2\pi i}\int_{-\infty}^{\infty} d\omega\ \frac{\omega}{\sinh^2\alpha_R}\left(\frac{\hbar\omega}{2k_BT}\right)^2 \mathrm{cosech}^2(\frac{\hbar\omega}{2k_BT})\ \left(\frac{1}{\sinh\alpha} - \frac{1}{\sinh\alpha^*}\right)\ . \tag{2.33}$$

In the high temperature limit we get $(\hbar\omega/2k_BT)^2\mathrm{cosech}^2(\hbar\omega/2k_BT) \ \rightarrow\ 1$. This gives the classical result for the thermal conductivity. In this limit a change of variables from ω to α_I leads to the following result for the thermal conductivity:

$$\begin{aligned} \kappa_{cl} &= \frac{2k_Bm\omega_c^2(2+\nu^2)}{\gamma\pi}\int_0^{\pi/2} d\alpha_I\ \frac{\sin^2(\alpha_I)}{(2+\nu^2)^2 - 4\cos^2(\alpha_I)} \\ &= \frac{k_Bm\omega_c^2}{\gamma\ (2+\nu^2+[\nu^2(4+\nu^2)]^{1/2})}\ , \end{aligned} \tag{2.34}$$

where $\nu = \omega_0/\omega_c$. This agrees with the result obtained in Ref. [40].

An interesting limiting case is the case of weak coupling to the reservoirs ($\gamma \to 0$). In this case Eq. (2.33) gives:

$$\begin{aligned} \kappa_{wc} &= \left(\frac{\hbar\omega_c^2}{k_B T}\right)^2 \frac{m k_B}{4\gamma\pi} \int_0^\pi d\alpha_I \ \sin^2\alpha_I \ \mathrm{cosech}^2(\frac{\hbar\omega_\alpha}{2k_B T}) \ , \qquad (2.35) \\ \text{where} \quad \omega_\alpha^2 &= \omega_0^2 + 2\omega_c^2[1-\cos(\alpha_I)] \ . \end{aligned}$$

This agrees with the result obtained in [22]. The temperature profile obtained by them differs from the linear form obtained by us and also by [40] and is incorrect. They nevertheless obtain the correct thermal conductivity, presumably because their derivation only uses the temperature profile close to the centre of the chain where it is again linear. In the low temperature limit, Eq. (2.35) gives $\kappa_{wc} \sim e^{-\hbar\omega_0/k_B T}/T^{1/2}$ for $\omega_0 \neq 0$ and $\kappa_{wc} \sim T$ for $\omega_0 = 0$. As noted in [22] the expression for thermal conductivity (in the weak scattering limit) is consistent with a simple relaxation-time form for the thermal conductivity. The temperature dependence of κ_{wc} then simply follows the temperature dependence of the specific heat of the 1-dimensional chain.

Finally we examine the general case where the coupling constant has a finite value. In Figs. (2.1,2.2) we plot the thermal conductivity as a function of temperature for two sets of parameter: (i) $\gamma/(m\omega_c) = 0.2, \nu = 0.5$ and (ii) $\gamma/(m\omega_c) = 0.2, \nu = 0.0$. The insets in the two figures show the low-temperature behaviour. As before, the low-temperature behaviour depends on whether or not there is an onsite potential. However we see that the form of the low-temperature behaviour is very different from the case of weak coupling. For small T it is easy to pull out the temperature dependence of the integral in Eq. (2.33) and we find that $\kappa \sim T^3$ for $\nu \neq 0$ and $\kappa \sim T^{1/2}$ for $\nu = 0$, in agreement with the numerical result shown in Figs. (2.1,2.2).

As an application of the LEGF results we have studied the problem of heat conduction in a one dimensional harmonic chain connected to self-consistent reservoirs [33]. The classical version of this problem was solved exactly by Bonetto *et al.* [40], using different methods. The quantum mechanical case was studied earlier by Vischer and Rich [22], and they obtained the thermal conductivity in the limit of weak coupling. The advantage of the present approach is that its implementation is simple and straightforward. We obtain a general expression for the thermal conductivity, which, in limiting cases, gives both the classical result in [40] and the weak-coupling result in [22]. We also find that, at low temperatures, the temperature dependence of thermal conductivity in the case of finite coupling is completely different from the weak coupling case. In the classical case, it was shown in [40] that the thermal conductivity of the harmonic chain with self-consistent reservoirs can also be obtained from the Kubo formula. An interesting problem would be to demonstrate this in the quantum-mechanical case. It is interesting to note that the self-consistent reservoirs are very similar to the Buttiker probes [24, 25] which have been used to model inelastic scatterering in electron transport. In the electron case, they lead to Ohm's law

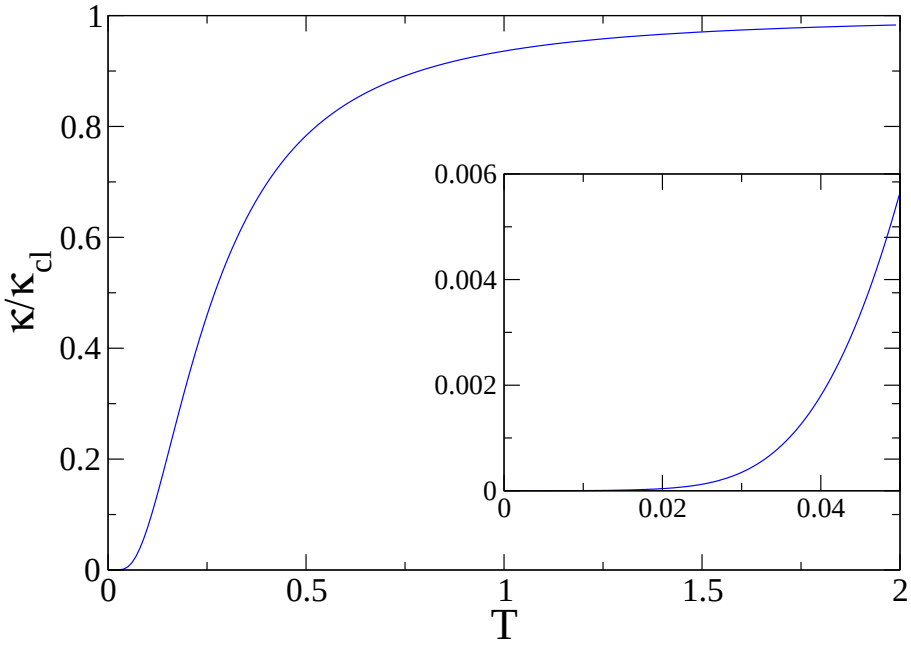

FIGURE 2.1: Plot of the scaled thermal conductivity as a function of temperature (in units of $\hbar\omega_c/k_B$) for $\nu = 0.5$. Inset shows the low temperature behaviour.

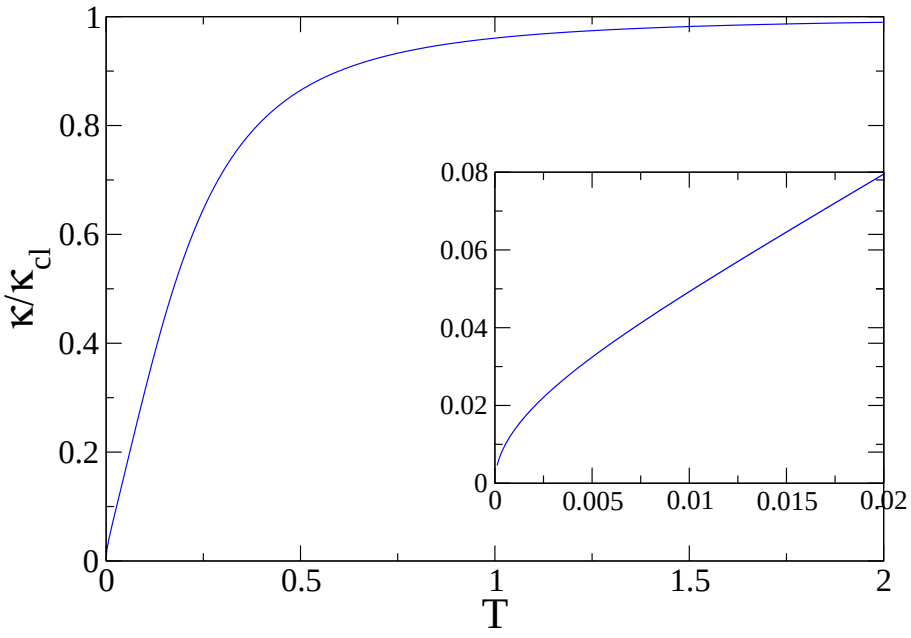

FIGURE 2.2: Plot of the scaled thermal conductivity as a function of temperature (in units of $\hbar\omega_c/k_B$) for $\nu = 0.0$. Inset shows the low temperature behaviour.

being satisfied, just as in the harmonic chain the introduction of self-consistent reservoirs leads to Fourier's law being satisfied. In fact, we have recently shown how one can obtain Ohm's law using self-consistent reservoirs modeled microscopically by noninteracting electron baths [65].

2.2.2 Finite chain: Crossover from ballistic to diffusive thermal transport

The transition from ballistic to diffusive dynamics in thermal and electrical transport has recently received a lot of attention. In a recent letter, Wang [75] has reported to have obtained quantum thermal transport from classical molecular dynamics using a generalised Langevin equation of motion. Based on a "quasiclassical approximation", the author claims to reconcile the quantum ballistic nature of thermal transport with diffusive one in a one-dimensional quartic on-site potential model. In Ref. [76], the authors have studied the transition from diffusive to ballistic dynamics for a class of finite quantum models by an application of the time-convolutionless projection operator technique. Here, through an exact analysis using quantum Langevin dynamics, we demonstrate the crossover from ballistic to diffusive thermal transport in a finite size harmonic chain connected to self-consistent reservoirs.

We consider again same self-consistent reservoir model as before. But now the coupling γ_l of the tth chain site to the Ohmic heat baths is given as, $\gamma_l = \gamma$ for $l = 1, N$ and $\gamma_l = \gamma'$ for $l = 2, 3..N-1$. This allows us to tune the coupling (γ') between self-consistent reservoirs and the chain sites without affecting the couplings at the end reservoirs. Also we assume here $m = \omega_c = \hbar = k_B = 1$ and $\omega_0 = 0$. With this little modification, we determine the temperature profile $\{T_l\}$ of the interior heat baths from the self-consistent condition. In FIG.2.3 we plot $\{T_l\}$ for different lengths of the chain for some fixed small value of γ'. In the limit $\gamma' << 1$ we find that the temperature profile scales as

$$\begin{aligned} T_1 &= T_L \ , \ T_N = T_R \text{ and} \\ T_l &= T_L + \delta + \frac{2\delta}{\ell}(l-2) \ \text{ for } \ l = 2, 3...N-1, \\ \text{with } \ \delta &= \frac{\Delta T}{2(1+N/\ell)} \ , \end{aligned} \tag{2.36}$$

where $\ell = 3/\gamma'$ and $\Delta T = T_R - T_L$. Here δ is the jump in the temperature at the boundaries. The above scaling relation can be derived from a persistent random walk model of phonons in analogy with the one for electrons [65]; here ℓ is interpreted as the mean free path of the phonons. We also plot $\{T_l\}$ profile in FIG.2.4 for fixed length $N = 256$ with different values of γ'. When γ' tends to zero (then ℓ goes to infinity), the heat transport in the chain is ballistic (becomes completely ballistic at $\gamma' = 0$), and the temperature profile is flat as shown in FIG.2.4. With increasing γ', the system transits through a mixed transport regime towards a diffusive one for

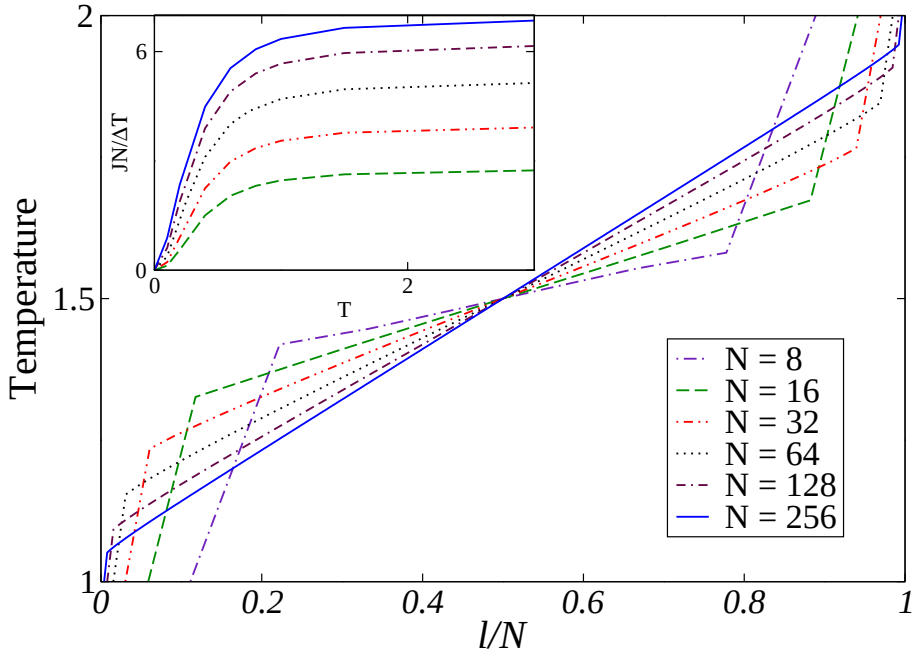

FIGURE 2.3: Plot of the temperature profile $\{T_l\}$ as a function of scaled length l/N for different N with $\gamma = 1.0$ and $\gamma' = 0.1$. The inset shows temperature dependence of scaled current for different N with above values of γ, γ'. Here mean free path $\ell = 30$.

sufficiently large value of γ' where ℓ is much smaller than the system size; then $\{T_l\}$ profile is linear. For larger value of γ', the temperature profile becomes linear for smaller system sizes.

The current through $(l, l+1)$ spring of the chain is given by Eq.(2.32)

$$\begin{aligned} & J_{l,l+1} = \langle x_l \dot{x}_{l+1} \rangle \\ = & -\sum_{m=1}^{N} \frac{\gamma_m T_m}{\pi} \int_{-\infty}^{\infty} d\omega \frac{\omega^3}{4T^2} \mathrm{cosech}^2(\frac{\omega}{2T}) Im[G_{lm} G^*_{l+1m}] \end{aligned} \tag{2.37}$$

Now, using the numerical solution for $\{T_l\}$, we first evalute the heat current with varying temperature for different N and γ', and plot it in the inset of FIG.2.3 and FIG.2.4 respectively. $J_{l,l+1}$ (call it J) is independent of l and we calculate it in the bulk for accuracy. Using the scaling form of $\{T_l\}$, we find that

$$J = \frac{\kappa(T)\ \Delta T}{(N+\ell)}\ , \tag{2.38}$$

where $\kappa(T)$ is the temperature dependent thermal conductivity of the infinite chain. Above current expression is exact for larger size of the chain, but for smaller size, there will be correction

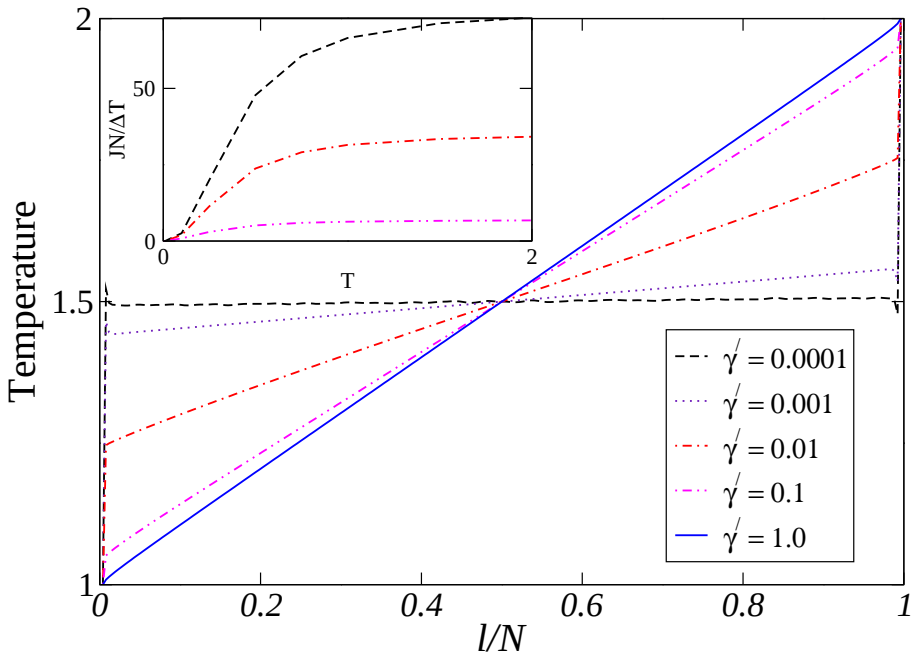

Figure 2.4: Plot of the temperature profile $\{T_l\}$ as a function of scaled length l/N for different γ' with $\gamma = 1.0$ and $N = 256$. The inset shows temperature dependence of scaled current for different γ' with above values of γ, N. Here mean free path $\ell = 3/\gamma'$.

from the boundaries. It clearly shows that, for $N >> \ell$, transport is diffusive, satisfying Fourier's law and in the opposite limit, the current is independent of N (ballistic). We clarify that the cross-over from ballistic to diffusive behaviour in transport depends on the effective length scale of the problem and can be controlled here by tuning ℓ, i.e., γ'. This model has similarity to the one-dimensional quartic on site potential model [75] if one identifies γ' with the strength of the quartic on site potential. But in the quartic on site potential model, the temperature and the strength of quartic potential are conjugate to each other, i.e., for a fixed strength of the quartic potential, increasing the temperature one can cross-over from ballistic to diffusive regime of transport; similarly for a constant temperature, changing the strength of quartic potential one can tune from ballistic to diffusive transport. But, in the case of the self-consistent reservoir model, the temperature and the strength of the coupling to the reservoirs (γ') are independent parameters, not affecting each other.

In conclusion, we have demonstrated both ballistic and diffusive regime of thermal transport within a single analysis of quantum Langevin dynamics. This is contrary to the remark made by author in Ref.[75]. As discussed nicely in [20, 77], it is a big challenge to derive Fourier's law for a system from microscopic Hamiltonian bulk dynamics. One can think of the problem as either (a) the system in microcanonical ensemble evolving towards equilibrium from an initial arbitrary

distribution and study the relaxation mechanism from different correlations like energy-energy, or, (b) the system is kept in a non-equlibrium steady state by connecting it at the boundaries with stochastic or mechanical reservoirs and then determine the size dependence of the steady state current . From a large number of numerical and a few analytical studies [14, 77], it is believed that the chaotic behaviour resulting from nonintegrability is an essential criterion for realizing Fourier's law in classical systems. Analogously from the numerical study of quantum systems with the coupling to external heat baths [78, 79] or without the baths [80], it is argued that the emergence of diffusive behaviour is related to onset of quantum chaos. Now, we try to analyse the underlying mechanism of getting diffusive behaviour in this self-consistent reservoir model. Originally, Bolsterli, Rich and Visscher [20] proposed the self-consistent reservoir model to incorporate phenomenologically the interactions of phonons with other degrees of freedom such as electron's charge and spin present in the physical system. Due to stochastic interactions with the internal reservoirs, the inherently non-ergodic harmonic chain becomes ergodic. Here, the self-consistent reservoirs provide the mechaism of scattering for phonons which is very much essential to get diffusive behaviour. It can also be posed in a different way that the self-consistent reservoirs act as the environment in a persistent random walk of phonon in a lane and break down the coherent nature of transport. In this context, this model is similar to the models of particle transport studied in [65], again with self-consistent particle reservoirs, and in [81] with heat baths modelling the dissipative environment. Now, we point out certain inconsistencies in the application of "quasiclassical approximation" in Ref.[75] which treats system classically neglecting all quantum fluctuations and random noises from the baths as quantum mechanically correlated. At high temperatures, where thermal fluctuations predominate over quantum fluctuations, the system is inherently classical. In the opposite limit, the strength of the anharmonicity in the quartic on site model is weaker if the temperature is lower. Here the anharmonicity can be treated perturbatively in an effectively harmonic system. So, in these two limits, the so called "quasiclassical approximation" is valid. But for intermediate temperatures, where the anharmonicity has significant strength, quantum fluctuations due to non-commutativity of the operators play an important role in lower dimensions. Then the "quasiclassical approximation" does not hold. Thus, though use of the "quasiclassical approximation" looks attractive, it has probably little application to real problems of quantum transport where phonon-phonon interaction is crucial. Finally, one main feature of our analysis is that the effective transport mean free path distinguishing ballistic regime from diffusive one emerges naturally in the study.

2.3 Heat transport in ordered harmonic lattices

We study here heat conduction across an ordered oscillator chain with harmonic interparticle interactions and also onsite harmonic potentials using LEGF method. RLL [43] considered the problem

of heat conduction across a one-dimensional ordered harmonic chain connected to stochastic heat baths at the two ends. The main results of this paper were: (i) the temperature in the bulk of the system was a constant equal to the mean of the two bath temperatures, (ii) the heat current approaches a constant value for large system sizes and an exact expression for this was obtained. RLL considered the case where only interparticle potentials were present. Nakazawa [44, 45] (N) extended these results to the case with a constant on site harmonic potential at all sites and also to higher dimensions.

The approach followed in both the RLL and N papers was to obtain the exact nonequilibrium stationary state measure which, for this quadratic problem, is a Gaussian distribution. A complete solution for the correlation matrix was obtained and from this one could obtain both the steady state temperature profile and the heat current. In our paper [42] we use LEGF to calculate the heat current in ordered harmonic lattices connected to Ohmic reservoirs (for a classical system, this is white noise Langevin dynamics). An advantage of the approach used here is that it can be easily generalized to the quantum mechanical regime [31, 33, 51–53]. Here we show how exact expressions for the asymptotic current ($N \to \infty$) can be obtained from this approach. We also briefly discuss the model in the quantum regime and extensions to higher dimensions.

The model we consider here is slightly different from the Nakazawa model. We consider the pinning potentials at the boundary sites to be different from the bulk sites. This allows us to obtain both the RLL and N results as limiting cases. Also it seems that this model more closely mimics the experimental situation. In experiments, the boundary sites would be interacting with fixed reservoirs which can be modeled by an effective spring constant that is expected to be different from the interparticle spring constant in the bulk. We also note here that the constant on site potential present along the wire relates to experimental situations such as that of heat transport in a molecular wire attached to a substrate, or, in the two-dimensional case, a monolayer on a substrate. Another example would be the heat current contribution from the optical modes of a polar crystal.

2.3.1 Model and Results in the Classical Case

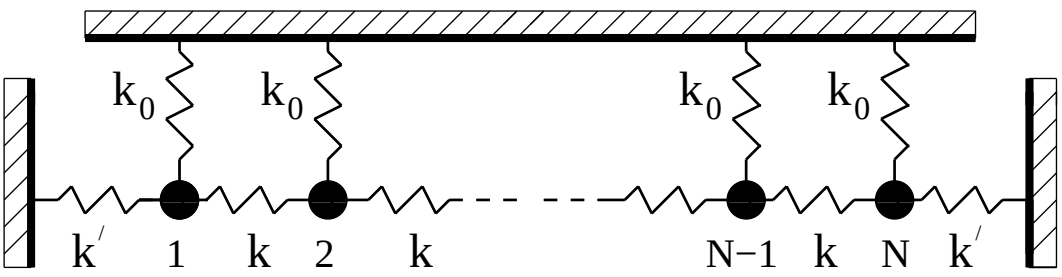

Figure 2.5: A schematic description of the model.

We consider N particles of equal masses m connected to each other by harmonic springs of equal spring constants k. The particles are also pinned by onsite quadratic potentials with strengths k_o at all sites except the boundary sites where the pinning strengths are $k_o + k'$ [see Fig. (2.5)]. The Hamiltonian of the harmonic chain is thus:

$$H = \sum_{l=1}^{N}[\frac{1}{2}m\dot{x}_l^2 + \frac{1}{2}k_o x_l^2] + \sum_{l=1}^{N-1}\frac{1}{2}k(x_{l+1} - x_l)^2 + \frac{1}{2}k'(x_1^2 + x_N^2)\ , \tag{2.39}$$

where x_l denotes the displacement of the particle at site l from its equilibrium position. The particles 1 and N at the two ends are immersed in heat baths at temperature T_L and T_R respectively. The heat baths are assumed to be modeled by Langevin equations corresponding to Ohmic baths. In the classical case the steady state heat current from left to right reservoir is given by [17, 67] :

$$\begin{aligned}
J_C &= \frac{k_B(T_L - T_R)}{4\pi}\int_{-\infty}^{\infty} d\omega\ \mathcal{T}_N(\omega), \qquad (2.40)\\
\text{where } \mathcal{T}_N(\omega) &= 4\gamma^2\omega^2|G_{1N}|^2\ ,\\
G &= [-m\omega^2 I + \Phi - \Sigma]^{-1}\ ,\\
\Phi_{lm} &= (k + k' + k_o)\ \delta_{l,m} - k\ \delta_{l,m-1} \qquad \text{for} \quad l = 1\ ,\\
&= -k\ \delta_{l,m+1} + (2k + k_o)\ \delta_{l,m} - k\ \delta_{l,m-1} \quad \text{for} \quad 2 \le l \le N-1\ ,\\
&= (k + k' + k_o)\ \delta_{l,m} - k\ \delta_{l,m+1} \qquad \text{for} \quad l = N\ ,\\
\Sigma_{lm} &= i\gamma\omega\delta_{lm}[\delta_{l1} + \delta_{lN}]\ ,
\end{aligned}$$

and I is a unit matrix. We now write $G = Z^{-1}/k$, where Z is a tri-diagonal matrix with $Z_{11} = Z_{NN} = (k + k_o + k' - m\omega^2 - i\gamma\omega)/k$, all other diagonal elements equal to $2 + k_o/k - m\omega^2/k$ and all off-diagonal elements equal to -1. Then it can be shown easily that $|G_{1N}(\omega)| = 1/(k\ |\Delta_N|)$ where Δ_N is the determinant of the matrix Z. This is straightforward to obtain and after some rearrangements we get:

$$\begin{aligned}
\Delta_N &= [a(q)\sin Nq + b(q)\cos Nq]/\sin q\ , \qquad (2.41)\\
\text{where } a(q) &= [2 - \frac{\gamma^2\omega^2}{k^2} + \frac{k'^2}{k^2} - \frac{2k'}{k}]\cos q + \frac{2k'}{k} - 2 - \frac{2i\gamma\omega}{k}[1 + (\frac{k'}{k} - 1)\cos q]\ ,\\
b(q) &= [\frac{\gamma^2\omega^2}{k^2} - \frac{k'^2}{k^2} + \frac{2k'}{k}]\sin q + \frac{2i\gamma\omega}{k}(\frac{k'}{k} - 1)\sin q\ ,
\end{aligned}$$

and q is given by the relation $2k\cos q = -m\omega^2 + k_o + 2k$. This relation implies that for frequencies outside the phonon band $k_o \le m\omega^2 \le k_o + 2k$ the wavevector q becomes imaginary and hence the transmission coefficient $\mathcal{T}(\omega)$ decays exponentially with N. Hence for large N we need only consider the range $0 < q < \pi$ and the current is given by:

$$J_C = \frac{2\gamma^2 k_B(T_L - T_R)}{k^2\pi}\int_0^{\pi} dq|\frac{d\omega}{dq}|\ \frac{\omega_q^2}{|\Delta_N|^2}\ , \tag{2.42}$$

with $m\omega_q^2 = k_o + 2k[1-\cos(q)]$. Now we state the following result:

$$\lim_{N\to\infty}\int_0^\pi dq \frac{g_1(q)}{1+g_2(q)\sin Nq} = \int_0^\pi dq \frac{g_1(q)}{[1-g_2^2(q)]^{1/2}} \ , \tag{2.43}$$

where $g_1(q)$ and $g_2(q)$ are any two well-behaved functions. This result can be proved by making an expansion of the factor $1/[1+g_2(q)\sin(Nq)]$ (valid for $|g|<1$ in the integration range), taking the $N\to\infty$ limit and resumming the resulting series. Noting now that Δ_N can be written as $|\Delta_N|^2 = (|a|^2+|b|^2)[1+r\sin(2Nq+\phi)]/[2\sin^2(q)]$ where $r\cos\phi = (ab^*+a^*b)/(|a|^2+|b|^2),\ r\sin\phi = (|b|^2-|a|^2)/(|a|^2+|b|^2)$, we see that Eq. (2.42) has the same structure as the left hand side of Eq. (2.43). Hence using Eq. (2.43), in the large N limit we can replace

$$\begin{aligned} \mathcal{T}_N &= \frac{4\gamma^2\omega^2}{k^2|\Delta_N|^2} = \frac{4\gamma^2\omega^2\sin^2 q}{[(|a|^2+|b|^2)/2][1+r\sin(2Nq+\phi)]} \\ \text{by}\ \ \mathcal{T}_\infty &= \frac{2k\gamma\omega\sin q}{2k^2-2kk'+k'^2+\gamma^2\omega^2+2k(k'-k)\cos q} \ . \end{aligned} \tag{2.44}$$

Thus we finally get from Eq. (2.42) :

$$\begin{aligned} J_C &= \frac{\gamma k^2 k_B(T_L-T_R)}{\pi m}\int_0^\pi \frac{\sin^2 q\ dq}{\Lambda-\Omega\cos q} \\ &= \frac{\gamma k^2 k_B(T_L-T_R)}{m\Omega^2}(\Lambda-\sqrt{\Lambda^2-\Omega^2}) \ , \\ \text{where}\ \ \Lambda &= 2k(k-k')+k'^2+\frac{(k_o+2k)\gamma^2}{m}\ \ \text{and}\ \ \Omega = 2k(k-k')+\frac{2k\gamma^2}{m} \ . \end{aligned} \tag{2.45}$$

Eq. (2.45) is the central result of this paper. We now show that two different special cases lead to the RLL and N results. First in the case of fixed ends and without onsite potentials, *i.e.* $k'=k$ and $k_o=0$, we recover the RLL result [43]:

$$J_C^{RLL} = \frac{kk_B(T_L-T_R)}{2\gamma}\Big[1+\frac{\nu}{2}-\frac{\nu}{2}\sqrt{1+\frac{4}{\nu}}\ \Big] \ \ \text{where}\ \ \nu = \frac{mk}{\gamma^2} \ . \tag{2.46}$$

The case $k'=k, k_o\neq 0$ can also be obtained using the RLL approach [82] and agrees with the result in Eq. (2.45). In the other case of free ends, *i.e.* $k'=0$, we get the N result [44, 45]:

$$J_C^N = \frac{k\gamma k_B(T_L-T_R)}{2(mk+\gamma^2)}\Big[1+\frac{\lambda}{2}-\frac{\lambda}{2}\sqrt{1+\frac{4}{\lambda}}\ \Big] \ \ \text{where}\ \ \lambda = \frac{k_o\gamma^2}{k(mk+\gamma^2)} \ . \tag{2.47}$$

2.3.2 Quantum mechanical case

In the quantum case the heat current across a chain described by the Hamiltonian Eq. (5.1) and connected to Ohmic heat baths is given by [33]:

$$J_Q = \frac{1}{4\pi}\int_{-\infty}^{\infty} d\omega\ \hbar\omega\mathcal{T}_N(\omega)[f(\omega,T_L)-f(\omega,T_R)] \ , \tag{2.48}$$

where $f(\omega,T) = 1/[e^{\hbar\omega/(k_BT)} - 1]$ is the phonon distribution function and $\mathcal{T}_N$ is as given in Eq. (2.40). Here we consider the linear response regime where the applied temperature difference $\Delta T = T_L - T_R << T$ with $T = (T_L + T_R)/2$. Expanding the phonon distribution functions $f(\omega, T_{L,R})$ about the mean temperature T we get the following expression for the current:

$$J_Q = \frac{k_B(T_L - T_R)}{4\pi} \int_{-\infty}^{\infty} d\omega \ \left(\frac{\hbar\omega}{2k_BT}\right)^2 \mathrm{cosech}^2\Big(\frac{\hbar\omega}{2k_BT}\Big) \ \mathcal{T}(\omega) \ . \tag{2.49}$$

We then proceed through the same asymptotic analysis as in the previous section and get, in the limit $N \to \infty$:

$$\begin{aligned} J_Q &= \frac{\gamma k^2\hbar^2(T_L - T_R)}{4\pi k_B m T^2} \int_0^{\pi} dq \frac{\sin^2 q}{\Lambda - \Omega\cos q} \ \omega_q^2 \ \mathrm{cosech}^2\Big(\frac{\hbar\omega_q}{2k_BT}\Big), \\ \text{where } \ \omega_q^2 &= [k_o + 2k(1-\cos q)]/m \ . \end{aligned} \tag{2.50}$$

We are not able to perform the above integral exactly. Numerically it is easy to obtain the integral for given parameter values and here we examine the temperature dependence of the current (note that in the classical case the current depends only on the temperature difference). In Fig.(2.6) we plot the current as a function of temperature in three different cases (i) $k' = k, k_o = 0$, (ii) $k' = 0, k_o = 0$ and (iii) $k' = 0, k_o \neq 0$. Particularly interesting is the low temperature ($T << \hbar(k/m)^{1/2}/k_B$) behaviour (shown in inset of Fig.(2.6)) which is very different for the three cases. The low temperature behaviour can be obtained analytically by examining the integrand at small q [83]. We then find for the three different cases: (i) $J_Q \sim T^3$, (ii) $J_Q \sim T$ and (iii) $J_Q \sim e^{-\hbar\omega_o/(k_BT)}/T^{1/2}$, where $\omega_o = (k_o/m)^{1/2}$.

2.3.3 Higher dimensions

Heat conduction in ordered harmonic lattices in more than one dimension was first considered by Nakazawa [45]. The problem can be reduced to an effectively one-dimensional problem. For the sake of completeness we reproduce their arguments here and also give the quantum generalization.

Let us consider a d-dimensional hypercubic lattice with lattice sites labelled by the vector $\mathbf{l} = \{l_\alpha\}, \alpha = 1, 2...d$, where each l_α takes values from 1 to L_α. The total number of lattice sites is thus $N = L_1L_2...L_d$. We assume that heat conduction takes place in the $\alpha = d$ direction. Periodic boundary conditions are imposed in the remaining $d-1$ transverse directions. The Hamiltonian is described by a scalar displacement $X_{\mathbf{l}}$ and as in the $1D$ case we consider nearest neighbour harmonic interactions with a spring constant k and harmonic onsite pinning at all sites with spring constant k_o. All boundary particles at $l_d = 1$ and $l_d = L_d$ are additionally pinned by harmonic springs with stiffness k' and follow Langevin dynamics corresponding to baths at temperatures T_L and T_R respectively.

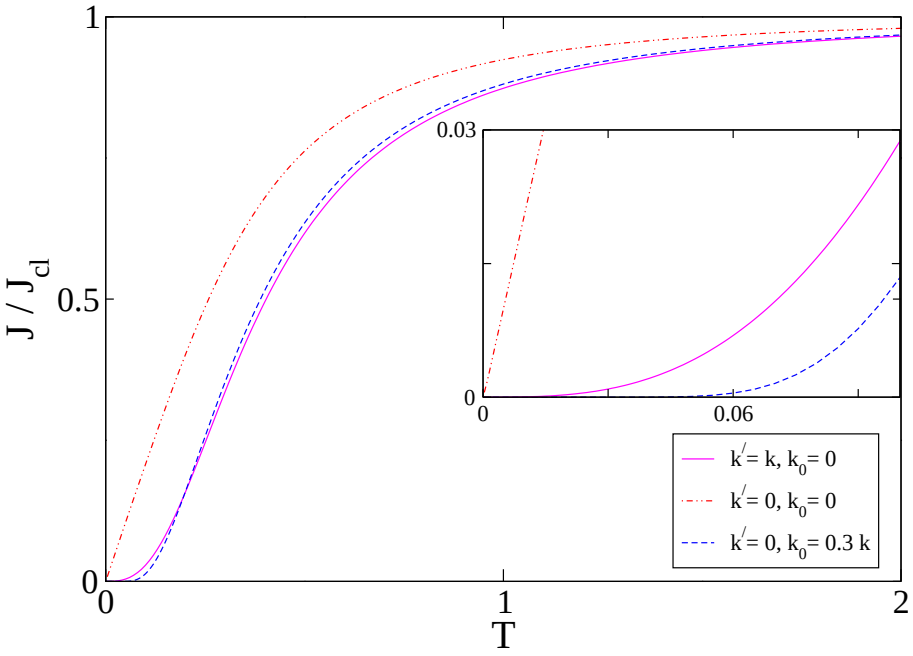

FIGURE 2.6: Plot of the scaled heat current with temperature (in units of $\hbar(k/m)^{1/2}/k_B$) for three different parameter regimes (see text). Inset shows the low temperature behaviour.

Let us write $\mathbf{l} = (\mathbf{l}_t, l_d)$ where $\mathbf{l}_t = (l_1, l_2 ... l_{d-1})$. Also let $\mathbf{q} = (q_1, q_2 ... q_{d-1})$ with $q_\alpha = 2\pi n/L_\alpha$ where n goes from 1 to L_α. Then defining variables

$$X_{l_d}(\mathbf{q}) = \frac{1}{L_1^{1/2} L_2^{1/2} ... L_{d-1}^{1/2}} \sum_{\mathbf{l}_t} X_{\mathbf{l}_t, l_d} e^{i\mathbf{q}.\mathbf{l}_t} \ , \tag{2.51}$$

one finds that, for each fixed $\mathbf{q}$, $X_{l_d}(\mathbf{q})$ ($l_d = 1, 2 ... L_d$) satisfy Langevin equations corresponding to the 1D Hamiltonian in Eq. (5.1) with the onsite spring constant k_o replaced by

$$\lambda(\mathbf{q}) = k_o + 2k[d - 1 - \sum_{\alpha=1,d-1} \cos(q_\alpha)] \ . \tag{2.52}$$

For $L_d \to \infty$, the heat current $J(\mathbf{q})$ for each mode with given $\mathbf{q}$ is then simply given by Eq.(2.45) with k_o replaced by $\lambda_{\mathbf{q}}$. In the quantum mechanical case we use Eq. (4.16). The heat current per bond is then given by:

$$J = \frac{1}{L_1 L_2 .... L_{d-1}} \sum_{\mathbf{q}} J(\mathbf{q}) \ . \tag{2.53}$$

Note that the result holds for finite lengths in the transverse direction. For infinite transverse lengths we get $J = \int ... \int_0^{2\pi} d\mathbf{q} J(\mathbf{q})/(2\pi)^{d-1}$.

2.3.4 Summary

In this section we have presented the results from our paper [42] where we have derived the exact formula for the heat current through an ordered harmonic chain in the limit of infinite system size. Our derivation is different from the methods used by RLL [43] and N [44, 45] and is for a slightly different version of the models studied by them. We have given the quantum mechanical generalization of the results. In that case one gets, in the linear response regime, a temperature dependent current with interesting low-temperature behaviour. We have also stated the results for the general d-dimensional case.